JOURNAL OF MATERIALS SCIENCE 2 (1967) 33–39

# $BeO{\cdot}Al_2O_3{\cdot}SiO_2$ System: Structural Relationships of Crystalline, Glassy, and Molten Beryl

E. F. RIEBLING, D. A. DUKE
*Research and Development Laboratories, Corning Glass Works, Corning, New York, USA*

*Received 16 September 1966*

Physical property measurements are reported for beryl glass and for three 60 mole % $SiO_2$ melts (including beryl) at temperatures above 1600° C. Electron micrographic evidence shows that beryl glass has undergone a two-liquid phase separation. Density measurements of this glass and its melt can be interpreted in terms of the dissociation of $Si_6O_{18}^{-12}$ rings as beryl melts incongruently. The presence of discrete $BeO_4$ tetrahedra and $AlO_6$ octahedra in molten beryl is suggested by the electrical conductance and viscosity data for these melts.

## 1. Introduction

Miller and Mercer [1] recently examined in detail the crystalline structural changes which took place upon slowly cooling beryl melts and during the devitrification of beryl glasses. The crystallisation sequence in each case was explained in terms of the relative crystal-lattice energies and the short-range order present in the glasses and melts. Phase relationships in the beryl system suggested a microheterogeneous melt with ion groupings dispersed in a silica-like framework. They also suggested that, by studying the structures of the glass and of the first crystalline phases to develop upon reheating, the coordination of ions in the melt could be presumed.

Work in this laboratory has demonstrated the value of high-temperature viscosity, density, and electrical conductance measurements in understanding the structure of molten silicates [2–4]. More recent work has shown that the compositional volume dependence of an oxide glass can be very similar to that observed for its melt [5].

The purpose of this paper is to attempt to correlate the crystallisation characteristics of beryl melts and glasses with the physical properties of the glasses and melts. The phase separation process in beryl glass will be described, and density, viscosity, and electrical conductance information will be presented for three melts containing 60 mole % $SiO_2$ which bracket the beryl composition. Experimental results will be discussed in terms of the various coordination polyhedra to be expected.

## 2. Experimental

Compositions of the melts made in this study are listed in table I and are plotted in fig. 1, the ternary system $BeO$-$Al_2O_3$-$SiO_2$. The liquidus temperatures estimated by Miller and Mercer

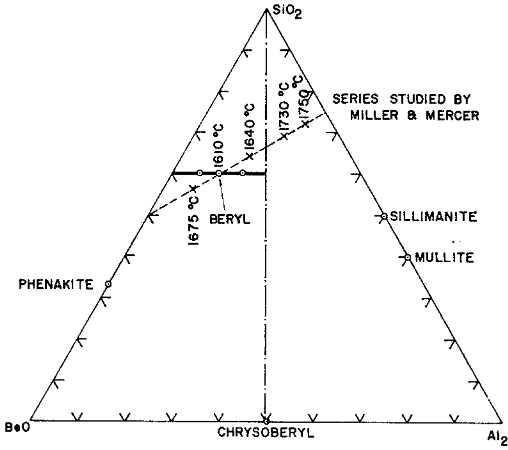

*Figure 1* Ternary diagram of the $BeO{\cdot}Al_2O_3{\cdot}SiO_2$ system showing the molar compositions studied (——⊙——) and those reported by Miller and Mercer (- - - X - - -).

TABLE I Chemical composition of $BeO \cdot Al_2O_3 \cdot SiO_2$ mixtures.

| Wt % BeO | $Al_2O_3$ | $SiO_2$ | Mole % BeO | $Al_2O_3$ | $SiO_2$ | Average molecular weight |
|---|---|---|---|---|---|---|
| 16.78 | 12.07 | 71.13 | 34 | 6 | 60 | 50.68 |
| 13.95 | 18.96 | 67.06* | 30 | 10 | 60 | 53.75 |
| 10.86 | 26.55 | 62.59 | 25 | 15 | 60 | 57.60 |

*Chemical analysis revealed 14.3 wt % BeO, 18.9 wt % $Al_2O_3$, and 67.2 wt % $SiO_2$.

for the compositions which they studied are also shown. Our compositions were kept at a constant 60 mole % $SiO_2$ to facilitate comparison with other ternary oxide systems and to simplify the structural interpretation of our data.

G C* grade BeO powder from the Brush Beryllium Co was added to dry mixtures of powdered, Baker reagent-grade $Al_2O_3$ and 200-mesh $SiO_2$ obtained from the Pennsylvania Glass Sand Co. A spectrographic analysis showed $Na_2O$ from 0.05 to 0.5% as the major impurity in the melts. 500 g batches were melted in platinum-rhodium crucibles for 16 h at 1750 to 1800° C. Small platinum-rhodium crucibles used in the subsequent viscosity and conductance studies were filled, and the remaining portion of each melt was poured into a patty which was annealed at 700° C. Since all of the samples crystallised to some extent upon normal cooling, significant quantities of glass were obtained by remelting and rolling ribbon approximately 0.3 mm thick through water-cooled rollers. The melt cooled slightly from 1800° C in the few seconds it took to remove the crucible from the furnace and start pouring into the rollers, at which time the melt was quenched to room temperature in a fraction of a second.

The glasses and their devitrification products were examined using X-ray diffraction and electron micrographic techniques. Crystalline phases that developed during cooling or upon reheating were determined by the powder X-ray method. Electron micrographs were taken of platinum-palladium, pre-shadowed, carbon replicas of samples which had been polished and then etched for 30 sec in 1/2% HF solution.

The viscometer-densitometer [6] and electrical conductance [7] instruments used in studying the molten oxides have previously been described. Chemical analysis showed that glass of the beryl composition was essentially stoichiometric (table I). Since the oxides used are not volatile and no significant condensation or alumina attack was noted during the high-temperature experimental runs, it was assumed that the composition of these melts remained that of the calculated oxide composition.

## 3. Results

### 3.1. Beryl Glass

All attempts to form a homogeneous, single-phase glass at the beryl stoichiometry were unsuccessful. Glass ribbon prepared by rolling the melt through water-cooled rollers was transparent and colourless, but a bluish opal glass formed in thicker sections of the ribbon. Figs. 2 and 3 show the phase separation which occurred in the transparent, and opal portions of the ribbon, respectively. The colourless ribbon, which visually appears as a uniform, homogeneous glass, exhibits phase-separated areas several hundred Ångströms in diameter. In contrast, the opalised sections have larger areas of phase separation, some of which are up to 1 $\mu$m in length.

### 3.2. Viscosity of Molten Beryl Compositions

The viscosity isotherms for several temperatures are shown in fig. 4 as a function of the Al/Be ratio. There was a decrease in the activation energy $\Delta H_n^{\pm}$ and a pronounced decrease in viscosity with the addition of trivalent aluminium for divalent beryllium.

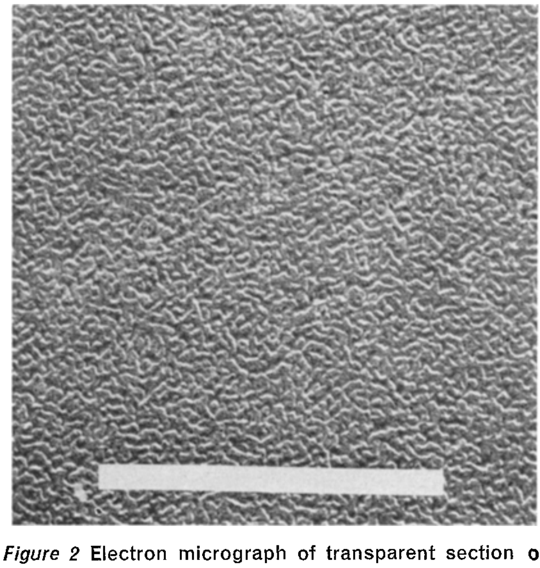

*Figure 2* Electron micrograph of transparent section of rapidly quenched beryl glass (white bar = 1 $\mu$m).

---

*G C (glass crystallised) grade BeO refers to the form of the powder before it is finally fired during preparation.

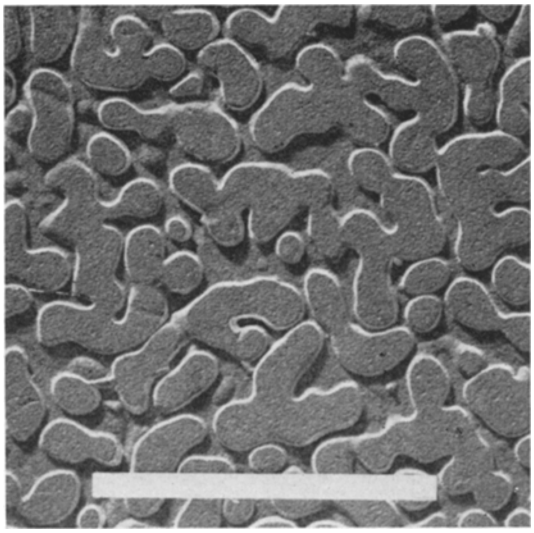

*Figure 3* Electron micrograph of opal section of rapidly quenched beryl glass (white bar = 1 μm).

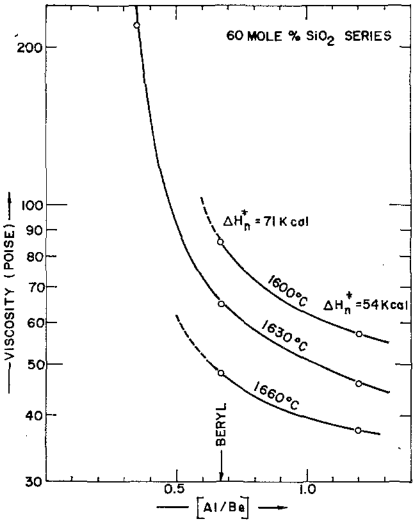

*Figure 4* Viscosity isotherms for 60 mole % $SiO_2$ melts as a function of the Al/Be ratio.

### 3.3. Electrical Conductance of Molten Beryl

A calibration change was initially encountered when the partially split mullite rod containing the 0.5 mm Pt-40% Rh electrode wires sagged at temperatures above 1700° C. Temperature and time were reduced in a subsequent experiment, and satisfactory post-run calibration data were obtained for the given electrode arrangement. The $\kappa$ (specific conductance) versus $\Omega$ measured curve used to calculate the specific conductance of the melt was an average of the before and after calibration data (uncertainty of $\pm 4\%$). The measured, high-temperature melt resistances were of the order of 30 to 40 $\Omega$ (lead resistance $\sim 2$ $\Omega$) and were quite reproducible during the run (fig. 5).

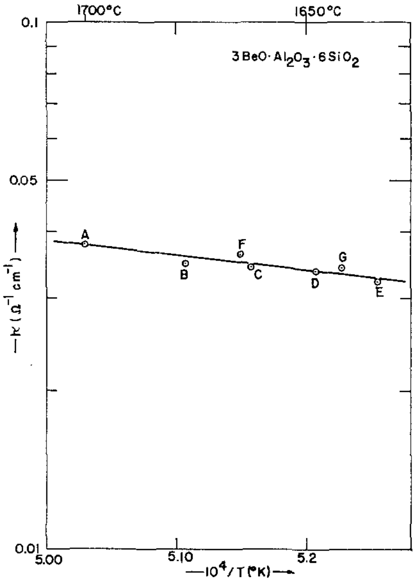

*Figure 5* Specific conductance ($\kappa$) of molten beryl as a function of $10^4/T$ (° K).

### 3.4. Density Determinations

The density of beryl glass, as determined with a microbalance technique, was found to be $2.445 \pm 0.0003$ g/cm$^3$ at 25° C. The calculated molar volume is shown on fig. 6 together with the experimentally determined 1630° C molar-volume isotherm for all three melts studied. There is a volume expansion that accompanies the substitution of $Al_2O_3$ for BeO at elevated temperatures.

## 4. Discussion

### 4.1. Phase Separation

Ganguli and Saha [8] noted the occurrence of an isotropic phase of lower refractive index within glass of the beryl composition and felt that this indicated liquid immiscibility. Miller and Mercer [1] also found evidence for immiscibility and related this phenomenon to disproportionation of the silicate anion.

Figs. 2 and 3 show in detail the actual nature of the phase separation which takes place in beryl glass. The highly irregular, interconnected,

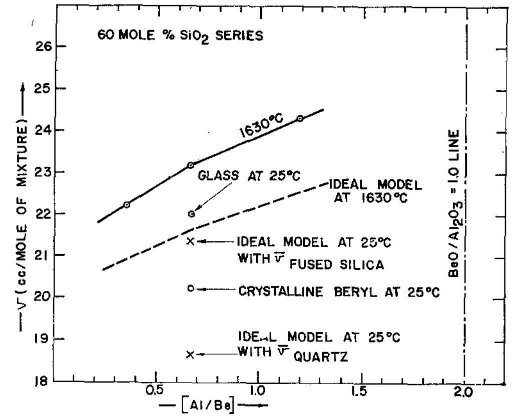

*Figure 6* Molar-volume isotherm (solid line) for $BeO \cdot Al_2O_3 \cdot SiO_2$ melts and the molar volume of beryl glass. Values for various volume models also shown.

two-phase structure observed is considered to be characteristic of spinodally separated glasses [9]. During the early stages of this type of microimmiscibility, there is a continuous composition gradient which becomes more distinct with time. This is in contrast to the "classical" nucleation and growth process in which two, distinct, composition regions are always present, resulting, in the early stages, in spherical droplets of the minor phase dispersed uniformly throughout the major phase.

The crystallisation sequence found can be interpreted in terms of the observed two-liquid phase separation. For example, shock heating of a quenched glass resulted in the crystallisation of the hybrid one phase [1]. Upon normal reheating, bromellite and mullite are the first crystalline phases identified. In the first case, the phase-separated regions are apparently not sufficiently developed, and only one crystalline phase, a beryllium aluminosilicate, occurs. With time, the composition regions become more distinct. Presumably, one glassy phase becomes enriched in BeO and the other is essentially an aluminosilicate.

Phase separation can arise from the competition of the cations for oxygen coordination. For example, in binary $Al_2O_3$-$SiO_2$ glasses, high $Al_2O_3$ concentrations result in a network based on both $AlO_4$ and $AlO_6$ and two-liquid phase separation occurs [10]. This dual coordination of aluminium ions is observed in the mineral sillimanite which has both four and six coordinated aluminium ions. When modifiers such as the alkali or alkaline earth ions are added to $Al_2O_3$-$SiO_2$ glasses, the $Al^{3+}$ ions are most stable in tetrahedral sites and immiscibility is reduced or eliminated. However, the addition of $Be^{2+}$ ions, with a higher field strength than other divalent ions, results in the formation of $BeO_4$ tetrahedra, relegating alumina to six-fold oxygen coordination, and phase separation once again takes place.

## 4.2. Viscosity

The viscosity and $\Delta H_n^{\pm}$ trends shown in fig. 4 are in direct contrast to the viscosity increase which has been observed for additions of $Al_2O_3$ to ternary sodium [2], potassium [11], magnesium [3], and calcium [12] aluminosilicate melts. The present results are indicative of two possible phenomena: (i) alumina enters the melt structure as $AlO_6$ octahedra – i.e. interstitial $AlO_6$ octahedra occur instead of the usual $AlO_4$ tetrahedra which enter the molten network in systems involving larger cations such as $Mg^{2+}$, $Ca^{2+}$, and $Na^+$; and/or (ii) the extensive three-corner-sharing, liquid network in the $BeO$-$SiO_2$ binary,* caused by the presence of network-forming $BeO_4$ tetrahedra, is loosened somewhat by the substitution of $AlO_4$ tetrahedra.

There is ample crystallographic evidence for the presence of $AlO_6$ octahedra in compositions where $Al_2O_3/BeO$ < unity. The beryl structure is formed by hexagonal rings of six silica tetrahedra, each tetrahedron sharing one oxygen to give the metasilicate ratio. The aluminium and beryllium atoms, which link together the oxygen atoms of the $Si_6O_{18}$ rings, are located between the hexagonal planes. Each $Al^{3+}$ is coordinated with a group of six oxygen atoms and each $Be^{2+}$ is four coordinated in a distorted tetrahedron [13]. Chrysoberyl ($Al_2BeO_4$) has an olivine-type structure with hexagonal close-packed oxygens producing an array of $BeO_4$ tetrahedra and $AlO_6$ octahedra [14].

There is also good reason to suspect that melts on or close to the $BeO \cdot SiO_2$ binary possess a strong tendency to produce three-dimensional, silica-like arrays. BeO has a wurtzite structure (tetrahedral coordination of both the cation and anion) formed by chains of corner-shared $BeO_4$ tetrahedra [15]. Phenakite ($Be_2SiO_4$) consists of a three-dimensional lattice of corner-

---

*The extrapolated viscosities for the $BeO$-$SiO_2$ binary are much larger than those observed for the $MgO$-$SiO_2$ melts [3]. For example, $\eta_{1600}$ for 40 mole % MgO silicate is about 30 poise, whereas $\eta_{1600}$ for 40 mole % BeO silicate > 200 poise, probably about $10^3$ to $10^4$ poise.

shared $BeO_4$ and $SiO_4$ tetrahedra [16]. This is undoubtedly due to the high field strength of $Be^{2+}$ and contrasts with ions like $Mg^{2+}$ and $Ca^{2+}$ which coordinate octahedrally in similar compositions.

The addition of $Al^{3+}$ for $Be^{2+}$ at the 60 mole % level, as would be expected, results in a viscosity decrease with $AlO_6$ octahedra being formed at the expense of $BeO_4$ tetrahedra. This is not the case in systems where $AlO_4$ tetrahedra are formed at the expense of $MgO_6$ octahedra, etc.

### 4.3. Cation Mobility

Analysis of the specific conductance data reveals that a melt with the beryl composition possesses the following equivalent conductances: $\Lambda_{1630} = 1.26\ \Omega^{-1}\ \text{eq}^{-1}\ \text{cm}^2$ and $\Lambda_{1700} = 1.41\ \Omega^{-1}\ \text{eq}^{-1}\ \text{cm}^2$. The $\Lambda$ values were calculated from: $\Lambda = 100\ \kappa M/(\rho m z x) = \Omega^{-1}\ \text{eq}^{-1}\ \text{cm}^2$, where $\kappa$ is the specific conductance in reciprocal ohm-centimetres, $M$ is the molecular weight of the oxide $M_xO_y$ responsible for conduction (in this case BeO), $\rho$ is the density, $m$ is the wt % BeO in the mixture, $z$ is the charge on Be, and $x$ is the number of Be atoms in BeO. This assumes that the $Be^{2+}$ conducts all of the electricity. The $Al^{3+}$ would not be expected to make a significant contribution to the observed conductivity because it is present in a smaller concentration and it possesses a smaller field strength than $Be^{2+}$.

Table II compares the equivalent conductance results calculated for molten beryl with data reported for other ternary silicate melts [4, 7] that contain similar amounts of $Al_2O_3$ and $SiO_2$. The magnesium aluminosilicate melt with about two-thirds the network modifier concentration of the beryl melt (with a similar $SiO_2$ content) has a cation mobility over four times larger.

TABLE II Electrical conductance data for ternary aluminosilicate melts.

| Mole % | | | | | | |
|---|---|---|---|---|---|---|
| BeO | $Na_2O$ | MgO | $Al_2O_3$ | $SiO_2$ | $\Lambda_{1700^\circ C}$ | $\Delta H_K^{\pm}$(kcal) |
| 30 | — | — | 10 | 60 | 1.41 | 12.1 |
| — | 20 | — | 15 | 65 | 70.0 | ~15.0 |
| — | 35 | — | 15 | 50 | 140.0 | ~14.0 |
| — | — | 18.7 | 17.4 | 63.9 | 6.18 | ~44.0 |

Although the activation energy for electrical conductance in the beryl melt is similar to that observed for other ternary oxide melts of equal $SiO_2$ content (table II), the cation mobility is much less than would be predicted [17] from field strength consideration of similarly charged cations (the smaller ion should possess the greatest mobility). Thus, while the activation process of cation movement is about the same as in other ternary melts, the structure of the beryl melt is such that cation mobility is severely impeded. The conductance results therefore suggest that the small, highly charged $Be^{2+}$ ions form $BeO_4$ tetrahedra in a three-dimensional array with $SiO_4$ tetrahedra.

### 4.4. Density

#### *4.4.1. General Considerations*

The melt molar-volume isotherm (fig. 6) can be interpreted using the synthetic, partial-molar-volume model technique previously used with other ternary silicate systems [2, 3]. This involves the assumption of one, relatively constant, partial molar volume (usually $\bar{v}_{SiO_2}$) in the following equation:

$$v = n_1\,\bar{v}_1 + n_2\,\bar{v}_2 + n_3\,\bar{v}_3$$
$$\text{(where } n = \text{mole fraction)}$$

The other $\bar{v}$ values are varied until $v_{calc}$ agrees reasonably well with $v_{obs}$. If the volume model so developed involves realistic coordination polyhedra that are consistent with available solid-state, viscosity, electrical conductance, infrared (etc.) information, then it can be concluded that reality has been approached. There follows a brief attempt to calculate $\bar{v}$ values to be used in the analysis of glass and melt volume data.

The room-temperature volume of BeO is 8.268 $cm^3$/mole and the room-temperature volume of chrysoberyl ($Al_2BeO_4$) is 17.12 $cm^3$/mole of mixture [18]. Use of the known volume of corundum ($AlO_6$ octahedra) and the above volume of bromellite ($BeO_4$ tetrahedra) permits the calculation of an assumed volume for chrysoberyl that is based on its structure [14]. This calculated volume is 16.98 $cm^3$ and agrees to within 0.5% of the experimental volume. Application of the same technique to hexagonal phenacite ($2BeO \cdot SiO_2$) involves the use of $\bar{v}_{quartz} = 22.67\ cm^3$ at 25° C [19], quartz being the stable configuration of $SiO_2$ at that temperature. This produces a calculated value of 13.02 $cm^3$ which is in good agreement with the experimental value of 12.31 $cm^3$. Thus, the solid-state volume calculations for two binary systems of the $BeO \cdot Al_2O_3 \cdot SiO_2$ system provide a coherent $\bar{v}$ basis for ternary volume calculations.

### *4.4.2. Glass*

A value of 20.20 cm$^3$/mole of beryl composition has been calculated for crystalline beryl at 25° C [20] and is plotted in fig. 6. This is for a material that contains $Si_6O_{18}{}^{-12}$ rings and interstitial $BeO_4$ tetrahedra and $AlO_6$ octahedra [13]. One model for beryl involves a $\bar{v}_{SiO_2}$ for silica. A second model involves the use of a $\bar{v}_{SiO_2}$ for fused quartz. The first volume model is close to the experimental volume for beryl glass (obtained with a density microbalance), while the second is closer to the volume of crystalline beryl (fig. 6).[*] Since it is presumed that no species have shifted coordination, it would appear that $\bar{v}_{SiO_2}$ for $Si_6O_{18}{}^{-12}$ rings in a crystalline compound lies between the ordered quartz-type array of $SiO_4$ tetrahedra and the disordered $SiO_4$ array found in fused silica. It can therefore be concluded from this data that $Si_6O_{18}{}^{-12}$ rings do not exist in either the glass or melt at the beryl composition. This agrees with studies which show that beryl melts incongruently [1, 8].

### *4.4.3. Melts*

The ideal volumes of the molten mixtures studied at 1630° C are represented by the dashed line in fig. 6. These were calculated with the aid of the following equation:

$$v = (n_{BeO})\,(8.65)^{\dagger} + (n_{Al_2O_3})\,(26.81) + (n_{SiO_2})\,(27.23)$$

where $\bar{v}_{SiO_2}$ is the high-temperature value for fused silica glass and the $n$ represents the mole fraction of each oxide. The positive experimental deviations from this simple mixing model vary between 7 and 10% and are therefore larger than the experimental uncertainties involved in determining the high-temperature melt volumes ($\approx < 1\%$).

Now, it can be estimated that a beryl crystal (melting point 1610° C) would have a volume of about 21.2 cm$^3$ at 1600° C ($20.2 + \approx 1.0$ cm$^3$ for a 5% thermal expansion from room temperature). This calculated, high-temperature, crystalline volume is about 2.0 cm$^3$ or 10% less than is experimentally observed for a melt of the beryl composition.[‡] It would appear that some structural rearrangement involving a more voluminous oxygen packing (~10% greater) occurs when beryl melts. This rearrangement could involve a breakdown of the $Si_6O_{18}{}^{-12}$ rings. This volume increase thus may not involve the introduction of holes such as occurs during the melting of simple ionic compounds such as NaCl and KCl.

Comparison of the above-estimated $\Delta v_{\mathrm{fusion}}$ for beryl with $\Delta v_{\mathrm{fusion}}$ for other silicates is revealing. Other ring-containing silicates like cordierite[§] ($AlSi_5O_{18}{}^{-13}$ rings in $2MgO{\cdot}2Al_2O_3{\cdot}5SiO_2$) and wollastonite ($Si_3O_9{}^{-6}$ rings in $CaO{\cdot}SiO_2$) appear to possess relatively small $\Delta v_{\mathrm{fusion}}$ values that are generally less than 1% [22, 23]. Thus, the melting behaviour of beryl is not characteristic of ring silicates. It is closer to that of most other silicates, which possess $\Delta v_{\mathrm{fusion}}$ values that generally vary from 5 to 15% [23]. For example, the feldspar albite ($Na_2O{\cdot}Al_2O_3{\cdot}6SiO_2$) possesses a 9 to 10% volume difference between its crystal and glass at 25° C [23]. Comparison of the $v_{\mathrm{crystal}}$ at 1100° C, calculated with the aid of the known expansion coefficient of about 5% [24], with the $v_{\mathrm{melt}}$ at that temperature [2] also indicates a 10% $\Delta v_{\mathrm{fusion}}$.

More work must certainly be completed upon the volume changes that accompany the melting of complex silicates before one can definitely correlate volume and structure changes at fusion points. Recent statements concerning the uncertain validity of the known pressure dependence of melting point for a number of silicates [25], from which $\Delta v_{\mathrm{fusion}}$ can be estimated, also suggest the need for more high-temperature fusion studies.

## 5. Conclusions

Two-liquid phase separation has been experimentally observed in a quenched, beryl-composition glass. This confirms and shows in detail the nature of the previously postulated immiscibility [8, 1]. The highly irregular, interconnected phases are characteristic of spinodally separated glass.

The viscosity, electrical conductance, and density measurements of beryl melts suggest the

---

[*] These comparisons are reasonable because most of the volume in a beryl composition is accounted for by $SiO_2$ (60 mole %). The largest term in the volume equation is the one for $SiO_2$. Hence, the calculations should be relatively sensitive to any significant change in $\bar{v}_{SiO_2}$.

[†] The known expansion coefficient of BeO ($\alpha_m = 9 \times 10^{-6}/°$ C for the 0 to 1400° C range) [21] was used to calculate $v_{BeO}$ at 1700° C.

[‡] Beryl glass also occupies about a 10% greater volume than does crystalline beryl at 25° C (fig. 6).

[§] Which also melts incongruently.

presence of $BeO_4$, $AlO_6$, and $SiO_4$ polyhedral groups, respectively. The density results for beryl glass and liquid suggest the absence of $Si_6O_{18}^{-12}$ rings and thus provide independent confirmation of the decomposition that occurs at the incongruent melting point of crystalline beryl. It has been concluded that the melting behaviour of beryl, which includes a large $\Delta v_{\text{fusion}}$, is more similar to network silicates than to other cyclosilicates such as cordierite and wollastonite.

## Acknowledgements

We would like to thank Mr G. B. Carrier for the electron micrographs, Mr E. P. Friebis for measuring the density of the beryl glass, and Mr P. E. Blaszyk and Mr D. W. Smith for assistance with the high-temperature measurements.

## References

1. R. P. MILLER and R. A. MERCER, *Mineral. Mag.* **35** (1965) 250.
2. E. F. RIEBLING, *J. Chem. Phys.* **44** (1966) 2857.
3. *Idem, Can. J. Chem.* **42** (1964) 2811.
4. *Idem, J. Electrochem. Soc.* **113** (1966) 920.
5. *Idem, Revue des Hautes Temperatures et des Refractaires*, to be published.
6. *Idem, Rev. Sci. Instr.* **34** (1963) 568.
7. E. F. RIEBLING and P. C. LOGEL, *ibid* **36** (1965) 425.
8. D. GANGULI and P. SAHA, *Central Glass and Ceramic Research Institute Bulletin* **12** (1965) 24.
9. J. H. CAHN and R. J. CHARLES, *Phys. Chem. Glasses* **6** (1965) 181.
10. J. F. MACDOWELL, *Ind. and Eng. Chem.* **58** (3) (1966) 41.
11. E. F. RIEBLING, unpublished results.
12. P. KOZAKEVITCH, *Rev. Met. Paris* **57** (1960) 147.
13. A. F. WELLS, "Structural Inorganic Chemistry", 3rd edition (Oxford University Press, 1962), pp. 797, 798.
14. R. W. G. WYCKOFF, "Crystal Structures", Volume II (Interscience, New York, 1960), Chapter VIII pp. 20, 21.
15. Reference 13, p. 426.
16. *Ibid*, p. 505.
17. E. F. RIEBLING and S. D. GABELNICK, *J. Electrochem. Soc.* **112** (1965) 822.
18. J. D. DONNAY and W. NOWASKI, "Crystal Data (Memoir 60)" (The Geological Society of America, New York, 1954), p. 288.
19. *Ibid*, p. 398.
20. *Ibid*, p. 409.
21. J. L. WHITE, "Physiochemical Measurements at High Temperatures", edited by J. O'M. Bockris, J. L. White, and J. D. Mackenzie (Academic Press, New York, 1959), p. 350.
22. W. SCHREYER and J. F. SCHAIRER, *J. Petrol.* **2** (1961) 324.
23. F. BIRCH, J. F. SCHAIRER, and H. C. SPICER, "Handbook of Physical Constants" (Geographical Society of America, Special Paper No. 36, New York, 1950), pp. 15, 184.
24. H. S. YODER and C. E. WEIR, *Am. J. Sci.* **249** (1951) 683.
25. F. G. SMITH, "Physical Geochemistry" (Addison-Wesley, 1963), pp. 201-203.